

Article

## Synthesis, Structure and Optical Properties of Di-m-benzihexaphyrins (1.1.0.0.0.0) and Di-m-benziheptaphyrins (1.0.1.0.0.0.0): Blackening of m-Phenylene Linked Dicarbaporphyrinoids by Simple p-Expansion

Thondikkal Sulfikarali, Jayaprakash Ajay, Cherumuttathu H Suresh, Padinjare Veetil Bijina, and Sabapathi Gokulnath

*J. Org. Chem.*, **Just Accepted Manuscript** • DOI: 10.1021/acs.joc.0c00754 • Publication Date (Web): 10 May 2020

Downloaded from [pubs.acs.org](https://pubs.acs.org) on May 14, 2020

### Just Accepted

“Just Accepted” manuscripts have been peer-reviewed and accepted for publication. They are posted online prior to technical editing, formatting for publication and author proofing. The American Chemical Society provides “Just Accepted” as a service to the research community to expedite the dissemination of scientific material as soon as possible after acceptance. “Just Accepted” manuscripts appear in full in PDF format accompanied by an HTML abstract. “Just Accepted” manuscripts have been fully peer reviewed, but should not be considered the official version of record. They are citable by the Digital Object Identifier (DOI®). “Just Accepted” is an optional service offered to authors. Therefore, the “Just Accepted” Web site may not include all articles that will be published in the journal. After a manuscript is technically edited and formatted, it will be removed from the “Just Accepted” Web site and published as an ASAP article. Note that technical editing may introduce minor changes to the manuscript text and/or graphics which could affect content, and all legal disclaimers and ethical guidelines that apply to the journal pertain. ACS cannot be held responsible for errors or consequences arising from the use of information contained in these “Just Accepted” manuscripts.

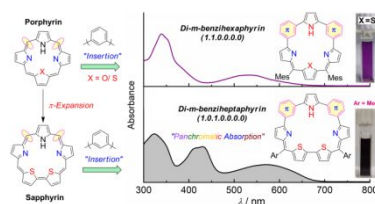
# Synthesis, Structure and Optical Properties of Di-*m*-benzihexaphyrins (1.1.0.0.0.0) and Di-*m*-benziheptaphyrins (1.0.1.0.0.0.0): Blackening of *m*-Phenylene Linked Dicarbaporphyrinoids by Simple $\pi$ -Expansion

Thondikkal Sulfikarali,<sup>a</sup> Jayaprakash Ajay,<sup>a</sup> Cherumuttathu H. Suresh,<sup>b</sup> Padinjare V. Bijina,<sup>b</sup> and Sabapathi Gokulnath\*<sup>a</sup>

<sup>a</sup>School of Chemistry, Indian Institute of Science Education and Research Thiruvananthapuram, Kerala-695551, India. E-mail: gokul@iisertvm.ac.in,

<sup>b</sup>Inorganic and Theoretical Chemistry Section, Chemical Science and Technology Division, CSIR-National Institute of Interdisciplinary Science and Technology, Trivandrum - 695019, Kerala, India

Supporting Information Placeholder



**ABSTRACT:** Acid catalyzed condensation of newly prepared di-*m*-benzipentapyrrane with appropriate mono- and diheterocyclic dialcohols selectively produced stable di-*m*-benzihexaphyrins and di-*m*-benziheptaphyrins with only two *meso*-carbon bridges. Single-crystal X-ray diffraction analyses reveal planar conformation with slight distortion of bridged phenylene rings. Despite the presence of *m*-phenylene units interrupting the global delocalization, the presence of bithiophene unit in di-*m*-benziheptaphyrins **3a-b** exhibit altered optical features covering the entire visible region (ca. 250 - 720 nm) exhibiting black dye property as a “metal-free” porphyrinoid.

## INTRODUCTION

Expansion of the porphyrin core through the introduction of various heterocyclic units or benzene units in place of one of the pyrrole rings may have interesting redox and optical properties.<sup>1</sup> Benziporphyrins are an important class of carbaporphyrinoids that encompass N<sub>3</sub>C core with unique ability to form organometallic species unlike regular porphyrins.<sup>2</sup> Majorly, two types of benziporphyrins namely *para*-benziporphyrin and *meta*-benziporphyrin are well explored.<sup>3</sup> However, the chemistry of *ortho*-benziporphyrins and their expanded analogues is being explored recently.<sup>4</sup> Meanwhile, benziporphyrinoids comprising one or more arene linkages in a *meta-ortho* (*m-o*), *meta-ortho-meta* (*m-o-m*) and *para-ortho-para* (*p-o-p*) fashion also known recently.<sup>4d-e</sup> The research groups of Latos-Grażyński and Lash have extensively investigated the synthetic methodologies and studied their spectral and electrochemical properties.<sup>5</sup> While *m*-benziporphyrin systems as in **I** are typically nonaromatic, aromaticity of such systems can be realized through keto-enol

tautomerism by appropriate substitutions on the benzene ring (Figure 1). On the other hand, *p*-benziporphyrins often show aromatic or antiaromatic features depending on the  $\pi$ -electrons involved in the annulenic conjugation.<sup>6</sup> Tetraphenyl *meta*-benziporphyrin **II** forms organometallic complexes with Pd<sup>2+</sup> and Pt<sup>2+</sup> salts. Upon addition of AgOAc, **II** undergoes selective acetoxylation at the internal carbon atom instead of silver metallation as inferred from X-ray crystallographic analysis.<sup>7</sup> In an earlier report, Ravikanth *et al.* reported a nonaromatic 24 $\pi$  dithia *m*-benzisapphyrin **III** through acid catalyzed condensation of benzitripyrrane with bithiophene diol.<sup>3a</sup> Structural analogue of porphyrin **IV** and its bimetallic complexes bearing *m*-phenylene unit with the alternating *meso* positions was synthesized by Corriu *et al.*<sup>8</sup> Recent interests into this area established several ways in tuning the optical and redox properties *via* reducing the *meso*-carbon bridges, introducing fused building blocks, and by incorporating phenylene units onto the macrocyclic core.<sup>9</sup> During such modifications, the presence of *meso*-carbons in these cyclic

structures often dictates their structure and conformational properties.<sup>3b-c,10</sup> A survey of

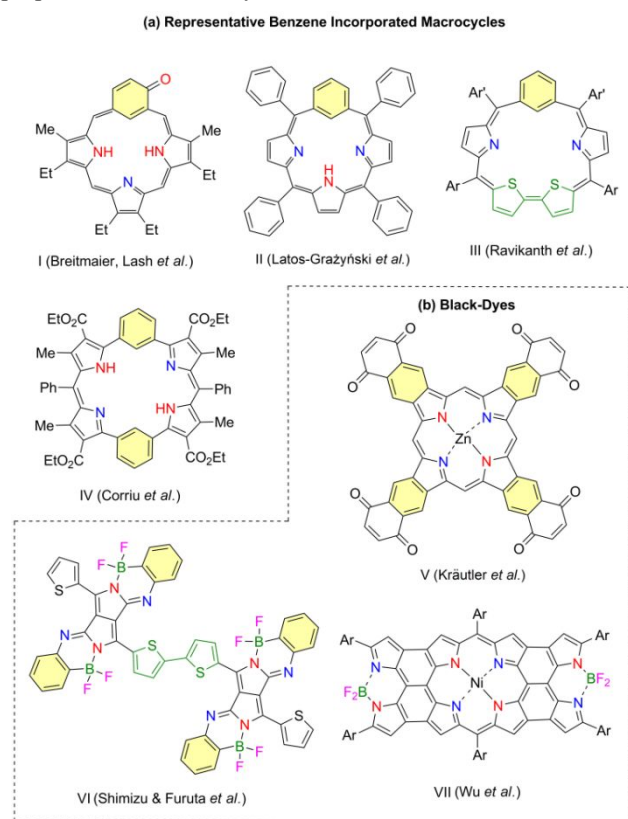


**Figure 1.** (a) Selected examples of benzoporphyrinoids and (b)  $\pi$ -extended chromophores exhibiting ‘black-dye’ property.

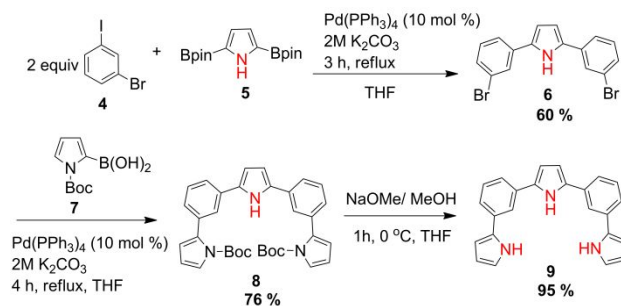
literature on carbaporphyrinoids reveals that expanded di-*m*-benzoporphyrins are ideal candidates that can provide altered optical properties through skeletal modifications.<sup>11</sup> Herein, we have attempted to further explore the relationship between the nature of conjugation with the optical and redox properties of these unique di-*m*-phenylene incorporated porphyrinoids.<sup>12</sup> We have devised a strategy to reduce the *meso*-carbon bridges by incorporating phenylene units in the place of two *meso*-positions of a porphyrin and sapphyrin derivatives, thereby restricting them to near planar conformation.<sup>13</sup> Recent interest in obtaining broad absorption bands in visible to near-IR has drawn significant attention due to the potential application with the aim of effective harvesting of solar energy.<sup>14</sup> Blackening of Zn<sup>2+</sup>-porphyrins **V** using peripherally fused  $\beta$ ,  $\beta'$ -quinono rings was reported by Krautler *et al.* and recent report by Furuta and Shimizu on blackening of aza-BODIPYs **VI** by simple dimerization unambiguously elucidated the significant role of linking units in achieving panchromatic absorption.<sup>15</sup> In order to push the absorption band towards near-IR region, Wu *et al.* prepared various porphyrin-fused BODIPY dye **VII** which displayed enhanced NIR absorption, due to the extended conjugation of porphyrin with fused BODIPY cores.<sup>16</sup> Interestingly, we found our bithiophene incorporated di-*m*-benzihexaphyrins **3a-b** exhibiting the optical absorption that covers the entire the UV to visible region with a ‘black-color’ in solution by simple  $\pi$ -expansion without involvement of metal

centres. This is in sharp contrast to our recent ‘black-dye’ *via* an expanded porphyrin hetero-*bis*-metal (Au<sup>III</sup>-Pd<sup>II</sup>) complex with absorption capabilities covering visible to near-IR region.<sup>14b</sup>

## RESULTS AND DISCUSSION

**Synthesis.** The *m*-phenylene incorporated macrocycles **1-3** were synthesized employing a sequence of steps, as shown in Scheme 1 and 2. Firstly, 2,5-bis(4,4,5,5-tetramethyl-1,3,2-dioxaborolan-2-yl)-1*H* pyrrole **5** was synthesized following a reported method.<sup>17</sup> Then, **5** was coupled with commercially available 1-bromo-3-iodobenzene **4** using 10 mol% Pd(PPh<sub>3</sub>)<sub>4</sub> affording 2,5-bis(3-bromophenyl)-1*H*-pyrrole **6**. Subsequently, compound **6** was further coupled with (1-(*tert*-butoxycarbonyl)-1*H*-pyrrol-2-yl)boronic acid **7** using a similar coupling method as described for **6** to yield *bis*-N-boc protected tripyrrole-like precursor **8** in 86% yield. In the next step, deprotection of **8** was successfully performed in the presence of NaOMe at 0 °C to provide a hitherto unknown tripyromethane-like precursor **9** as a stable brown powder in 95% yield. These compounds were characterized by <sup>1</sup>H and <sup>13</sup>C NMR spectroscopic methods. The heterocyclic diols, such as furan diol **10a**, thiophene diol **10b**, and bithiophene diols **11a-b**, were prepared by following the reported procedures.<sup>18</sup>

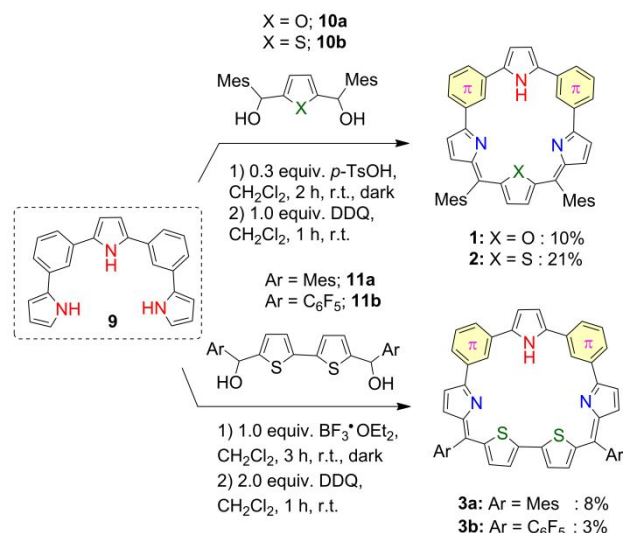
**Scheme 1.** Synthesis of *m*-phenylene linked key building blocks **6** and **9**.



To accomplish the synthesis of di-*m*-benzihexaphyrins **1-2**, equimolar amounts of **9** with appropriate heterocyclic diols **10a-b** were condensed in the presence of a catalytic amount of *para*-toluenesulfonic acid (*p*-TsOH) under inert atmosphere for 3 h, followed by an oxidation with 1.0 equiv of DDQ in open air at room temperature (Scheme 2) provided the macrocycles **1** and **2** in 10 and 21% yields, respectively. Initial characterization of **1** and **2** was done using MALDI-TOF analysis and proved the exact composition of these macrocycles (Figure S1-4 to S1-7). Then, similar condensation reaction with biheterocyclic dicarbinols such as **11a-b**<sup>18b</sup> did not provide the expected macrocycles **3a-b**. However, to our surprise, changing the acid catalyst to BF<sub>3</sub>•Et<sub>2</sub>O and using 2.0 equivalents of DDQ provided the target macrocycles **3a-b** in 8 and 3% yields, respectively. Although the yields of the macrocycles **3a-b** are low, the reaction was found to be reproducible. Attempts to reduce macrocycles **1** and **2** using NaBH<sub>4</sub> did not yield any reduced products, whereas macrocycles **3a-b** underwent reduction as indicated by sharp color changes. However, they

instantaneously reverted back to their oxidized forms during column chromatographic purification.

**Scheme 2.** Synthesis of di-*m*-benzihexaphyrins **1-2** and di-*m*-benziheptaphyrins **3a-b**.



**NMR Characterization.** The  $^1\text{H}$  NMR spectrum of **2** in  $\text{CDCl}_3$  showed two sharp singlets at 9.08 and 6.68 ppm for ring A and D, respectively (Figure 2a). A broad singlet at 11.06 ppm for the NH proton suggests the  $C_2$ -symmetric structure preserved in solution. Interestingly, two sets of doublets between 7.41 to 7.69 ppm and a triplet at 7.43 ppm were observed and found to correlate with each other in  $^1\text{H}$ - $^1\text{H}$  COSY spectrum due to the outer  $\beta$ -CHs of ring B (Figure S2-7). Signals corresponding to ring C of imino type pyrroles exhibit two well resolved doublets at 7.10 and 6.91 ppm. Similar spectral pattern was observed for **3a** with bithiophene incorporated macrocycle bearing two *meso*-mesityl rings (Figure

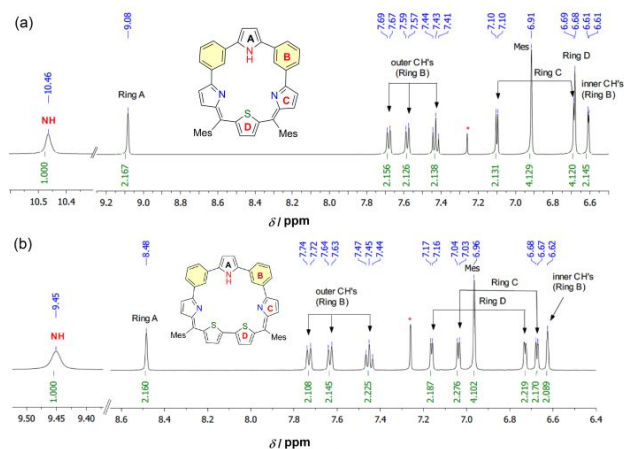


**Figure 2.** Comparison of  $^1\text{H}$  NMR spectra of macrocycles (a) **2** and (b) **3a** recorded in  $\text{CDCl}_3$ . Selected region is shown. \* denotes residual  $\text{CHCl}_3$  signal.

2b). Overall, the spectral features in all these macrocycles resemble typical non-aromatic characteristics, as observed in *m*-benzoporphyrioids<sup>3b</sup> and their expanded analogues.<sup>19</sup>

**Crystallographic Studies.** The structures of **2** and **3a** have been confirmed by single crystal X-ray diffraction analysis as shown in Figure 3, and crystallographic data are given in Table S3-1. Suitable single crystals of **2** were obtained by slow diffusion of methanol into chloroform solution of **2** at room temperature. Similarly, slow diffusion of *n*-hexane into the chloroform solution of **3a** provided X-ray quality crystals of **3a**. Both crystallize in monoclinic crystal lattice with  $P2_1/n$  space group. Structures of **2** and **3a** consist of a slightly twisted tripyrrin part directly connected with phenylene-pyrrole-phenylene linkage in an almost symmetric manner as shown in Figures 3a-b. The crystal structure **2** revealed that two molecules are present in the asymmetric unit. The heterocyclic rings and two benzene rings (ring A-F) were deviated with dihedral angles of 19.53°, 18.51°, 16.09°, 8.20°, 16.48°, and 13.31° with respect to the mean plane (C6-C9-C22-C36), thus giving a curved conformation. Similar heterocyclic rings and benzene rings (ring A-G) deviations were observed in **3a** with dihedral angles of 27.52°, 15.94°, 11.51°, 14.02°, 17.70°,

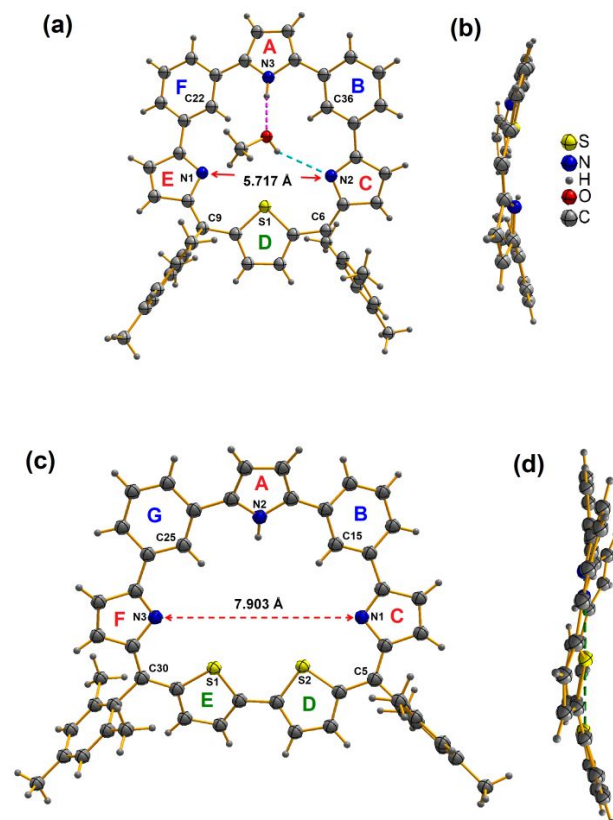


**Figure 3.** Single crystal X-ray structures of **2** with top (a) and side view (b) and **3a** with top (c) and side view (d). For clarity, solvent molecule and mesityl rings have been omitted in the side views. Ellipsoids are shown at 50% probability level.

17.79°, and 1.98° with respect to the mean plane (C5-C15-C25-C30), thus giving a saddle-like conformation (Figure S3-3 and S3-4, SI). The decreased ring deviation of one of the benzene rings can be attributed to the minimized steric congestion between the adjacent pyrrole rings. The N---N distance inside the macrocyclic core of **2** is 5.717 Å, which is larger in **3a** having 7.903 Å due to the core expansion by the incorporation of bithiophene units. Significantly, the DFT optimized structures of both **2** and **3a** resemble closely to those of single crystal X-ray structures without ring inverted conformations (Figure S6-7 and S6-8, SI).

**Optical properties.** The UV-Vis absorption spectrum of **1** in CH<sub>2</sub>Cl<sub>2</sub> exhibits the Soret-like and a Q-like band at 337 and 497 nm (Figure 4), respectively, which are blue-shifted in comparison to those of **2** with the Soret-like band at 339 nm and Q-like band at 532 nm. On the other hand, the fluorescence emission of **1** shows two maxima at 594 and 630 nm on excitation at 337 nm in CH<sub>2</sub>Cl<sub>2</sub>. Upon protonation using dilute CF<sub>3</sub>COOH in CH<sub>2</sub>Cl<sub>2</sub>, **1** and **2** showed a decreased intensity of the bands at ca. 330 nm with appearance of new featureless bands from 400–600 nm (Figure S4-2). On the other hand, the absorption features of bithiophene incorporated macrocycle **3a** and **3b** are perturbed in different ways. **3a** displays two broad bands at 323 and 429 nm with a low energy band at 570 nm. Similarly, **3b** exhibits absorption spectral features as that of **3a**. The additional band at 429 nm in **3a** and 414 nm in **3b**

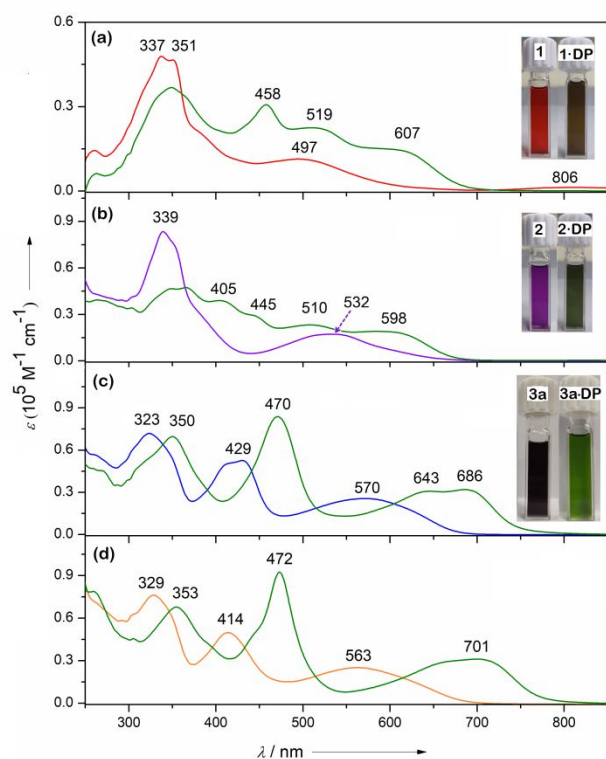


**Figure 4.** Comparison of absorption spectra of macrocycles (a) **1** (b) **2** (c) **3a** and (d) **3b** and their respective protonated forms (green trace) recorded in CH<sub>2</sub>Cl<sub>2</sub>. Inset: Solution colors of respective macrocycles in CH<sub>2</sub>Cl<sub>2</sub>. The solution colors of **3a-b** and their protonated forms are not distinguishable.

responsible for covering the absorption to the whole visible region, thus giving the ‘black-dye’ property of these macrocycles in solution.<sup>15</sup> In the drop-cast film state, both **3a** and **3b** exhibit slight broadening and red-shift of the main along with the bathochromically shifted absorption is due to the effective interchromophore interactions via the bithiophene moiety in coplanar conformations. These features could be absorption bands, denoting the formation of the  $\pi$ -stacked aggregates (Fig. S4-6).

**Redox Properties.** The estimation of the HOMO-LUMO energy gap for all these macrocycles were investigated via cyclic voltammetry in dichloromethane using 0.1 M tetrabutylammonium hexafluorophosphate as a supporting electrolyte. The estimated electrochemical HOMO–LUMO gap of 1.59 V for **1** and 1.67 V for **2** (Figure 5 and S5-1 in SI) were obtained from one irreversible oxidation wave at 0.71 V, a reversible reduction peak at -0.88 V for **1**, whereas for **2**, two irreversible waves for oxidation process at 0.80 V and 1.00 V with a reversible reduction peak at ca. -0.88 V and a quasi-

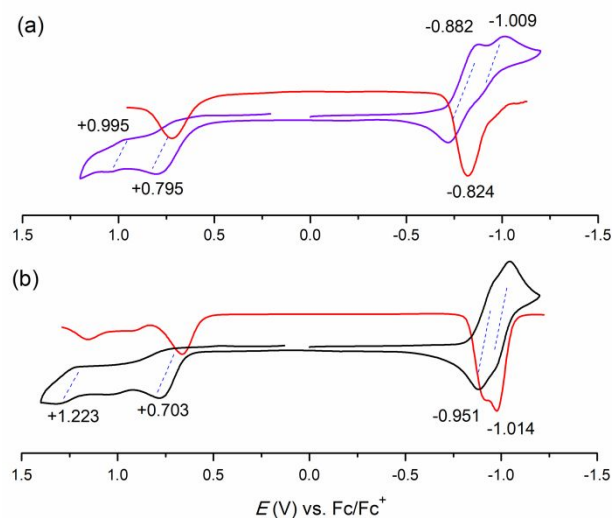


**Figure 5.** Cyclic voltammograms of **2** and **3a** (top to bottom; 1 mM in CH<sub>2</sub>Cl<sub>2</sub>, 0.1 M n-Bu<sub>4</sub>NPF<sub>6</sub>, scan rate 0.1 mV s<sup>-1</sup>, glassy carbon electrode). Respective Differential Pulse Voltammograms are shown in red trace.

**Table 1.** Electrochemical<sup>a</sup> and optical data<sup>b</sup> for macrocycles **1**, **2**, **3a** and **3b**

	$E^{1/2}_{ox.2}$ [V]	$E^{1/2}_{ox.1}$ [V]	$E^{1/2}_{red.1}$ [V]	$E^{1/2}_{red.2}$ [V]	$\Delta E_{opt}^b$ [eV]	$\Delta E_{DFT}$ [eV]
<b>1</b>	0.86 <sup>c</sup>	0.71 <sup>c</sup>	-0.88 <sup>d</sup>	-	2.49	4.11
<b>2</b>	0.99	0.79	-0.88	-1.01	2.33	3.87
<b>3a</b>	1.22	0.70	-0.95	-1.01	2.17	4.07
<b>3b</b>	1.23	0.81	-0.78 <sup>d</sup>	-	2.20	3.94

<sup>a</sup>Potentials[V] vs ferrocene/ferrocenium ion. Scan rate 0.1 Vs<sup>-1</sup>; working electrode, glassy carbon; counter electrode, Pt wire; supporting electrolyte, 0.1 M n-Bu<sub>4</sub>NPF<sub>6</sub>; reference electrode, saturated calomel electrode. <sup>c</sup>Determined by differential pulse voltammetry. <sup>d</sup>two-electron reduction process.

reversible peak at -1.01 V for the reduction process are observed. On the other hand, macrocycle **3a**, exhibits two reversible waves for reduction process at ca. -0.95 V and -1.01 V while two irreversible oxidation peaks are observed at 0.7 V and 1.22 V with an electrochemical HOMO-LUMO gap of 1.65 V (Table 1 and Table S5-1 in SI). Compound **3b** exhibit similar redox profile providing a slight reduction in the HOMO-LUMO gap of 1.59 V suggesting that no significant change in the redox properties was realized on going from electron rich mesityl rings to the electron withdrawing pentafluorophenyl substituents.

**DFT Calculations.**<sup>21</sup> The analysis of frontier molecular orbitals (FMOs) reveals that the HOMO of macrocycle **1** and **2** are comparable, whereas the LUMO of **2** is found to be stabilized to some extent as compared to that of **1** (Figure 6). This leads to slight decrease in the band gap ( $\Delta E = 3.87$  eV) for macrocycle **2** compared to that of **1** ( $\Delta E = 4.10$  eV), support the red shift in the absorption spectra of **2**. Further, comparison of the molecular orbital energies for the ring expanded derivatives **3a** and **3b** reveals that both the HOMO and LUMO of **3b** are

indicated that the heterocyclic rings were slightly deviated from planarity as obtained from single crystal X-ray structure (Figure 3). Analysis of selected FMOs of macrocycle **1** and **2** indicated that the HOMOs in both were localized mainly on the di-*m*-benzopyrrole core (Figure 6). The LUMOs were densely distributed on furan or thiophene core, leaving no orbital densities on *meso* substituents, whereas it is only distributed on di-*m*-benzopyrrole core of **3b** due to the electron withdrawing of *meso*-C<sub>6</sub>F<sub>5</sub> groups (Figure S6-9). Strikingly, LUMOs for both **3a** and **3b** were localized on bithiophene and the adjacent pyrrole rings.

## CONCLUSIONS

We herein presented three di-*m*-phenylene incorporated hexaphyrin and heptaphyrin-like structures exhibiting non-aromatic features. Effective localization is not realized due to the interrupted conjugation at the phenylene moieties as supported by their spectral and theoretical investigations. Our current results demonstrate that the replacement of thiophene or furan with bithiophene unit enable the effective tuning of the absorption characteristics. This synthetic strategy could be

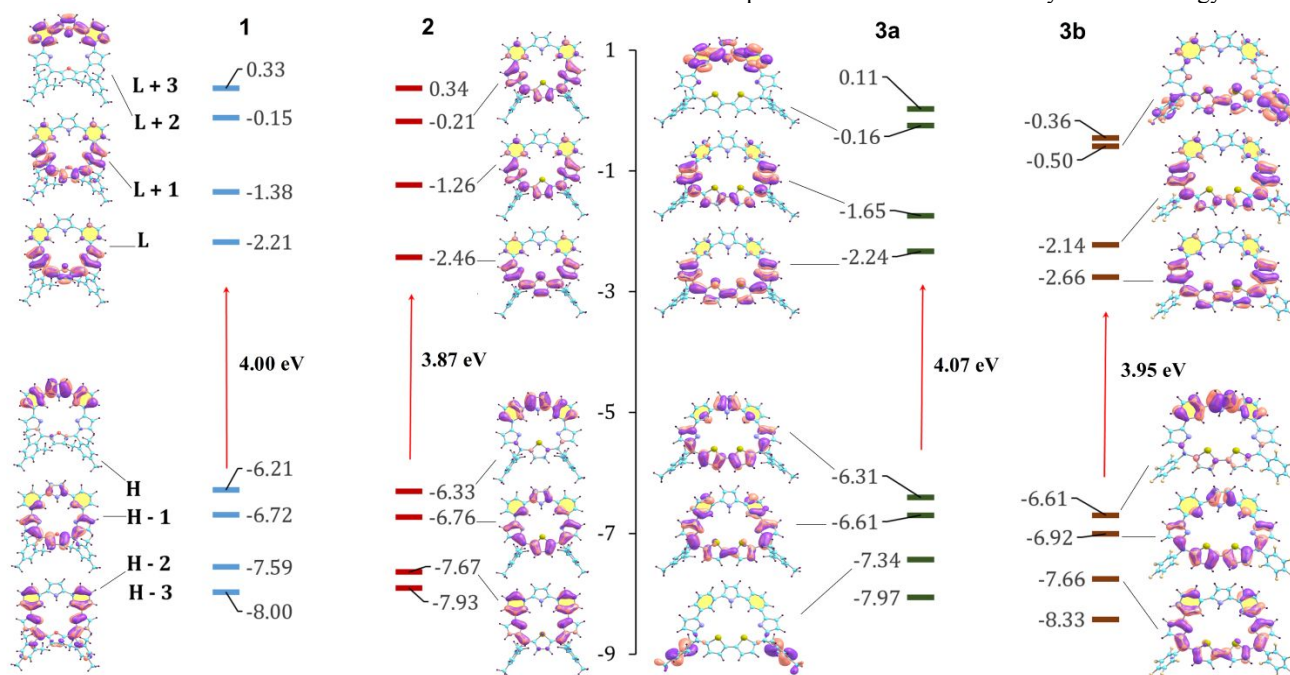


**Figure 6.** Energy level diagrams of **1**, **2**, **3a**, **3b** with selected molecular orbitals

stabilized as compared to **3a**. However the band gap is comparable (4.07 eV for **3a** vs 3.95 eV for **3b**), which is consistent with their optical and redox characteristics. The NICS(0) values for **1** and **2** were found to be 2.2 and 2.6 ppm, respectively (Figures S6-1 and S6-2). In addition, the random current density flow of the ACID plots of **1** and **2** validate the nonaromatic character of the molecules (Figure S6-5). Similar low positive NICS(0) values (1.9 ppm for **3a-b**) and ACID plots confirm the nonaromaticity in these macrocycles (Figure S6-3, S6-4 and S6-6). The S<sub>0</sub> (ground) state optimized geometries are presented in Figure S6-7. The DFT optimized structures for **3a**

successfully used for further modification of the porphyrin structure or for assembly of larger covalent porphyrin arrays. The atypical optical and electronic properties of these macrocycles are likely to be systematically tunable by varying the linkages between the *m*-arene and heterocyclic subunits. Presently, activating the inner CH's of the phenylene rings of these macrocycles towards organometallic complexes is underway in our laboratory.

## EXPERIMENTAL SECTION

### Materials and Methods

The reagents and materials for the synthesis were used as obtained from Sigma-Aldrich and Alfa-Aesar chemical suppliers. All solvents were purified and dried by standard methods prior to use. Silica gel column chromatography was performed on Wakogel C-200 and C-300. Alumina column chromatography was performed on Active alumina (basic). Thin-layer chromatography (TLC) was carried out on aluminum sheets coated with silica gel 60 F254 (Merck 5554). The visualization of spots was achieved using UV light ( $\lambda_{\text{max}} = 254 \text{ nm}$  and  $366 \text{ nm}$ ) or a  $\text{KMnO}_4$  staining solution (3.0 g  $\text{KMnO}_4$ , 20 g  $\text{K}_2\text{CO}_3$ , 5.0 mL (5.0%)  $\text{NaOH}$ , 300 mL  $\text{H}_2\text{O}$ ). Recrystallized samples of porphyrinoids were utilized for all the spectroscopic measurements.  $^1\text{H}$  NMR (500 or 700 MHz) and  $^{13}\text{C}$  NMR (125.8 MHz) spectra were recorded on Bruker 400 (AVANCE III) and INOVA 500 (Varian) spectrometer. Chemical shifts are reported in parts per million (ppm,  $\delta = \text{scale}$ ) relative to the signal of tetramethylsilane ( $\delta = 0.00 \text{ ppm}$ ).  $^1\text{H}$  NMR spectra are referenced to tetramethylsilane as an internal standard or the residual solvent signal of the respective solvent:  $\text{CDCl}_3$ :  $\delta = 7.26 \text{ ppm}$ ,  $\text{CD}_2\text{Cl}_2$ :  $\delta = 5.32 \text{ ppm}$ .  $^{13}\text{C}$  NMR spectra are referenced to the following signals:  $\text{CDCl}_3$ :  $\delta = 77.26 \text{ ppm}$ . The following abbreviations for multiplicities were used: singlet (s), broad singlet (br), doublet (d), triplet (t), quartet (q), multiplet (m) and combinations thereof, i.e. doublet of doublets (dd). Coupling constants ( $J$ ) are given in Hertz [Hz]. Structural assignments were made with additional information from COSY experiments. HRMS spectra were measured on a Thermo Fisher Scientific inc. Exactive or LCQ Advantage via electron spray ionization (ESI) or atmospheric pressure chemical ionization (APCI) with an orbitrap analyser. Cyclic and differential-pulse voltammetric measurements were performed on a PC-controlled electrochemical analyzer (CH instruments model CHI620C) using a conventional three-electrode cell for samples (1 mM) dissolved in dry  $\text{CH}_2\text{Cl}_2$  containing 0.1 M  $n\text{-Bu}_4\text{NPF}_6$  (TBAPF<sub>6</sub>) as the supporting electrolyte. Measurements were carried out under an argon atmosphere. A glassy carbon working electrode, a calomel reference electrode and platinum wire counter electrode were used in all electrochemical experiments. The potential were calibrated using the ferrocenium/ferrocene couple. The optical absorption spectra were recorded on a Shimadzu (Model UV-3600) spectrophotometer. Concentrations of solutions are *ca.* to be  $1 \times 10^{-6} \text{ M}$  (porphyrin Soret band) and  $5 \times 10^{-5} \text{ M}$  (porphyrin Q-bands). Single crystal X-ray intensity data were collected on a Bruker KAPPA APEXII diffractometer in omega and phi scan mode,  $\text{MoK}\alpha = 0.71073 \text{ \AA}$  at 298 K.

### Synthetic Manipulations

Synthesis of 2,5-Bis(4,4,5,5-tetramethyl-1,3,2-dioxaborolan-2-yl)-1H-pyrrole<sup>22</sup> and *N*-(*tert*-Butoxycarbonyl)-pyrrole-2-boronic acid (*N*-Boc-Py-B(OH)<sub>2</sub>)<sup>23</sup> were prepared by slightly modifying the previously reported procedures.

**2,5-bis(3-bromophenyl)-1H-pyrrole (6).** A flame-dried flask was charged with **5**<sup>22</sup> (1.0 g, 3.13 mmol), 1-bromo-3-iodobenzene (**4**) (1.19 g, 9.39 mmol), 2M  $\text{K}_2\text{CO}_3$  (4.31 g, 31.3 mmol),  $\text{Pd}(\text{PPh}_3)_4$  (0.36 g, 0.31 mmol, 10 mol%). The flask was evacuated and backfilled with argon and degassed anhydrous THF (20 mL) was added. The reaction mixture was refluxed for 3 h using an oil bath with constant stirring. The reaction was allowed to cool to room temperature and quenched by addition of  $\text{NaHCO}_3$  (30 mL). The layers were separated, and the aqueous layer was extracted with  $\text{CH}_2\text{Cl}_2$  ( $5 \times 20 \text{ mL}$ ). The organic extracts were dried over  $\text{MgSO}_4$ , filtered, and the solvent was removed in vacuo. The crude product was purified *via* flash column chromatography on silica gel (15%  $\text{CH}_2\text{Cl}_2/\text{Hexane}$ ) provided **6** (0.701 g, 60% yield) as a stable white solid.

Analytical data for **6**:  $^1\text{H}$  NMR (500 MHz,  $\text{CDCl}_3$ ):  $\delta = 8.56$  (s, 1H), 7.68 (s, 2H), 7.47 (d,  $J = 7.7 \text{ Hz}$ , 2H), 7.38 (d,  $J = 7.9 \text{ Hz}$ , 2H), 7.28 (d,  $J = 7.7 \text{ Hz}$ , 2H), 6.61 (s, 2H);  $^{13}\text{C}\{^1\text{H}\}$  NMR (126 MHz,  $\text{CDCl}_3$ )  $\delta = 134.4, 132.4, 130.7, 129.6, 127.0, 123.4, 122.7, 109.3$ ; HRMS (ESI<sup>+</sup>):  $m/z$  calcd. for  $\text{C}_{16}\text{H}_{12}\text{Br}_2\text{N}^+$  375.9331 [M+H]<sup>+</sup>, found 375.8978.

**Di-*tert*-butyl 2,2'-((1H-pyrrole-2,5-diyl)bis(3,1-phenylene))bis(1H-pyrrole-1-carboxylate) (8).** A flame-dried flask was charged with **6** (0.5 g, 1.33 mmol), *N*-(*tert*-butoxycarbonyl)-pyrrole-2-boronic acid **7**<sup>23</sup> (0.84 g, 4 mmol), 2 M  $\text{K}_2\text{CO}_3$  (3.67 g, 26.6 mmol),  $\text{Pd}(\text{PPh}_3)_4$  (0.15 g, 0.13 mmol, 10 mol%). The flask was evacuated and backfilled with argon and degassed anhydrous THF (20 mL) was added. The reaction mixture was refluxed for 4 h using an oil bath with constant stirring. The reaction was allowed to cool to room temperature and quenched by addition of  $\text{H}_2\text{O}$  (30 mL). The layers were separated, and the aqueous layer was extracted with  $\text{CH}_2\text{Cl}_2$  ( $5 \times 20 \text{ mL}$ ). The organic extracts were dried over  $\text{MgSO}_4$ , filtered, and the solvent was removed in vacuo. The crude product was purified *via* flash column chromatography on silica gel (40%  $\text{CH}_2\text{Cl}_2/\text{Hexane}$ ) provided **8** (1.1 g, 76% yield) as a stable off-white solid.

Analytical data for **8**:  $^1\text{H}$  NMR (500 MHz,  $\text{CDCl}_3$ ):  $\delta = 8.72$  (s, 1H), 7.48 (s, 2H), 7.43 (d,  $J = 7.6 \text{ Hz}$ , 2H), 7.36 (s, 2H), 7.30 (t,  $J = 7.6 \text{ Hz}$ , 2H), 7.16 (d,  $J = 7.4 \text{ Hz}$ , 2H), 6.56 (s, 2H), 6.21 (s, 4H), 1.33 (s, 18H).  $^{13}\text{C}\{^1\text{H}\}$  NMR (126 MHz,  $\text{CDCl}_3$ )  $\delta = 149.6, 135.3, 134.9, 133.2, 132.0, 128.3, 127.4, 124.8, 122.8, 122.7, 114.7, 110.8, 108.1, 83.9, 27.8$ ; HRMS (ESI<sup>+</sup>):  $m/z$  calcd. for  $\text{C}_{34}\text{H}_{36}\text{N}_3\text{O}_4^+$  550.2700 [M+H]<sup>+</sup>, found 550.2687;  $m/z$  calcd. for  $\text{C}_{34}\text{H}_{35}\text{N}_3\text{O}_4\text{Na}^+$  572.2525 [M+Na]<sup>+</sup>, found 572.2507.

**2,5-Bis(3-(1H-pyrrol-2-yl)phenyl)-1H-pyrrole (9).** When a methanolic-THF solution of **8** (0.25 g, 0.45 mmol) was treated with  $\text{NaOMe}$  (0.49 g, 9.1 mmol) at 0 °C for 1 h, smooth deprotection was observed by monitoring the disappearance of the starting material by TLC. The reaction was quenched by adding ice-cold water (20 mL). The organic layer was extracted using diethyl ether

(2 x 20 mL) followed by the removal of solvent under vacuum afforded **9** in a quantitative yield. This product seems sensitive to heat and light. Hence, this key building block was used instantaneously in the subsequent condensation step.

Analytical data for **9**:  $^1\text{H}$  NMR (500 MHz,  $\text{CDCl}_3$ ):  $\delta$  = 8.73 (s, 1H), 8.54 (s, 2H), 7.58 (s, 2H), 7.32 (s, 4H), 7.27 (s, 2H), 6.83 (s, 2H), 6.57 (d,  $J$  = 12.9 Hz, 4H), 6.30 (s, 2H);  $^{13}\text{C}\{^1\text{H}\}$  NMR (126 MHz,  $\text{CDCl}_3$ )  $\delta$  = 133.7, 133.4, 133.2, 132.1, 129.7, 122.2, 122.0, 119.7, 119.3, 110.4, 108.4, 106.5; HRMS (ESI):  $m/z$  calcd. for  $\text{C}_{24}\text{H}_{18}\text{N}_3^+$   $[\text{M}-\text{H}]^+$ . 348.1495 found 348.1335.

**Di-*m*-benzihexaphyrins (1): 9** (0.10 g, 0.286 mmol) and furan-2,5-diylbis(mesitylmethanol) **10a**<sup>18a</sup> (0.10 g, 0.286 mmol) was dissolved in dry  $\text{CH}_2\text{Cl}_2$  (250 mL). After stirring for 5 min under a  $\text{N}_2$  atmosphere, *para*-toluenesulfonic acid (*p*-TsOH) (0.016 g, 0.085 mmol) was added and the mixture was stirred for 2 h at room temperature, and then DDQ (0.065 g, 0.286 mmol) was added. After stirring for an additional 1 h, the mixture was treated with 2-3 drops of  $\text{Et}_3\text{N}$  and filtered through short alumina column until the eluent becomes colorless. The solvent was then removed under vacuum and the crude product was purified by silica gel column chromatography using a mixture of  $\text{CH}_2\text{Cl}_2$  in hexane (1:1). The resulting solid was recrystallized from  $\text{CH}_2\text{Cl}_2$ /Hexane afforded **1** in 10% (19 mg) yield.

Analytical data for **1**:  $^1\text{H}$  NMR (500 MHz,  $\text{CDCl}_3$ ):  $\delta$  = 11.06 (s, 1H, NH), 9.12 (s, 2H), 7.63 (d,  $J$  = 7.8 Hz, 2H), 7.48 (d,  $J$  = 7.6 Hz, 2H), 7.36 (t,  $J$  = 7.7 Hz, 2H), 7.22 (s, 2H), 7.16 (d,  $J$  = 4.7 Hz, 2H), 6.83 (s, 4H), 6.77 (d,  $J$  = 4.7 Hz, 2H), 6.59 (d,  $J$  = 2.3 Hz, 2H), 2.25 (s, 6H), 2.11 (s, 13H);  $^{13}\text{C}\{^1\text{H}\}$  NMR (126 MHz,  $\text{CDCl}_3$ )  $\delta$  = 171.9, 158.6, 154.9, 138.3, 138.2, 137.4, 134.9, 134.1, 133.7, 133.5, 132.0, 129.1, 128.4, 128.2, 126.7, 125.3, 123.5, 123.1, 107.1, 32.2, 30.0, 29.6, 22.9, 21.4, 20.6, 14.4. UV/Vis/NIR ( $\text{CH}_2\text{Cl}_2$ ):  $\lambda_{\text{max}}/\text{nm}$  ( $\log \epsilon$  [ $\text{mol}^{-1} \text{dm}^3 \text{cm}^{-1}$ ]): 337 (4.68), 351 (4.67), 497 (4.07). MALDI-TOF:  $m/z$  calcd for  $\text{C}_{48}\text{H}_{40}\text{N}_3\text{O}$ : 674.309  $[\text{M}+\text{H}]^+$ ; found: 674.349.

**Di-*m*-benzihexaphyrins (2):** The above mentioned procedure was followed by using **9** (0.1 g, 0.286 mmol), thiophene-2,5-diylbis(mesitylmethanol) **10b**<sup>18a</sup> (0.10 g, 0.286 mmol), *p*-TsOH (0.016 g, 0.085 mmol) and then DDQ (0.065 g, 0.286 mmol). The dark orange colored fraction was eluted with 60%  $\text{CH}_2\text{Cl}_2$ /Hexane afforded **2** as dark violet solids, yield 41 mg (21%).

Analytical data for **2**:  $^1\text{H}$  NMR (500 MHz,  $\text{CDCl}_3$ ):  $\delta$  = 10.46 (s, 1H, NH), 9.08 (s, 2H), 7.68 (d,  $J$  = 7.7 Hz, 2H), 7.58 (d,  $J$  = 7.6 Hz, 2H), 7.43 (t,  $J$  = 7.7 Hz, 2H), 7.10 (d,  $J$  = 4.7 Hz, 2H), 6.91 (s, 4H), 6.68 (d,  $J$  = 3.2 Hz, 4H), 6.61 (d,  $J$  = 2.3 Hz, 2H), 2.34 (s, 6H), 2.10 (s, 12H);  $^{13}\text{C}\{^1\text{H}\}$  NMR (126 MHz,  $\text{CDCl}_3$ )  $\delta$  = 172.6, 154.8, 148.7, 141.4, 138.2, 138.0, 137.0, 136.02, 134.9, 133.3, 133.0, 129.4,

128.3, 126.9, 126.6, 126.2, 122.7, 107.3, 21.3, 20.2. UV/Vis/NIR ( $\text{CH}_2\text{Cl}_2$ ):  $\lambda_{\text{max}}/\text{nm}$  ( $\log \epsilon$  [ $\text{mol}^{-1} \text{dm}^3 \text{cm}^{-1}$ ]): 339 (4.92), 532 (4.24). MALDI-TOF:  $m/z$  calcd for  $\text{C}_{48}\text{H}_{41}\text{N}_3\text{S}$ : 691.286  $[\text{M}+2\text{H}]^+$ ; found: 691.308.

**Di-*m*-benziheptaphyrins (3a):** An oven dried flask was charged with **9** (0.1 g, 0.286 mmol) and [2,2'-bithiophene]-5,5'-diylbis(mesitylmethanol) **11a**<sup>18b</sup> (0.13 g, 0.286 mmol). The flask was evacuated and backfilled with argon and degassed  $\text{CH}_2\text{Cl}_2$  250 mL. Then,  $\text{BF}_3\cdot\text{OEt}_2$  (36  $\mu\text{L}$ , 0.286 mmol) was added using a microsyringe and the mixture was stirred for 3 h at room temperature followed by the addition of DDQ (0.13 g, 0.572 mmol). After stirring for an additional 1 h in open air, the mixture was treated with 2-3 drops of  $\text{Et}_3\text{N}$  and filtered through short alumina column until the eluent becomes colorless. The solvent was then removed under vacuum. Column chromatography (silica gel, hexane/ $\text{CH}_2\text{Cl}_2$ : 1/0 to 1/6) afforded and the reasonably pure product. The resulting solid was recrystallized from  $\text{CH}_2\text{Cl}_2$ /Hexane to give macrocycle **3a** as dark green solids in 8% yield (16 mg).

Analytical data for **3a**:  $^1\text{H}$  NMR (500 MHz,  $\text{CDCl}_3$ ):  $\delta$  = 9.45 (s, 1H, NH), 8.48 (s, 2H), 7.73 (d,  $J$  = 7.8 Hz, 2H), 7.63 (d,  $J$  = 7.6 Hz, 2H), 7.45 (t,  $J$  = 7.7 Hz, 2H), 7.16 (d,  $J$  = 4.0 Hz, 2H), 7.04 (d,  $J$  = 4.6 Hz, 2H), 6.96 (s, 4H), 6.73 (d,  $J$  = 4.0 Hz, 2H), 6.67 (d,  $J$  = 4.5 Hz, 2H), 6.62 (s, 2H), 2.38 (s, 6H), 2.14 (s, 12H);  $^{13}\text{C}\{^1\text{H}\}$  NMR (126 MHz,  $\text{CDCl}_3$ )  $\delta$  = 171.3, 153.6, 148.2, 141.5, 141.3, 138.0, 137.1, 136.5, 135.7, 135.6, 135.3, 134.2, 129.2, 128.9, 128.3, 127.6, 127.4, 125.7, 121.6, 109.9, 21.4, 20.2. UV/Vis/NIR ( $\text{CH}_2\text{Cl}_2$ ):  $\lambda_{\text{max}}/\text{nm}$  ( $\log \epsilon$  [ $\text{mol}^{-1} \text{dm}^3 \text{cm}^{-1}$ ]): 323 (4.86), 430 (4.72), 570 (4.42). MALDI-TOF:  $m/z$  calcd for  $\text{C}_{52}\text{H}_{42}\text{N}_3\text{S}_2$ : 772.274  $[\text{M}+\text{H}]^+$ ; found: 772.312.

**Di-*m*-benziheptaphyrins (3b):** Compound **3b** was synthesized using **9** (0.1 g, 0.286 mmol) and [2,2'-bithiophene]-5,5'-diylbis(perfluorophenyl)methanol) **11b**<sup>18b</sup> (0.16 g, 0.286 mmol) by following the above procedure for compound **3a**. Yield 3% (6 mg).

Analytical data for **3b**:  $^1\text{H}$  NMR (500 MHz,  $\text{CDCl}_3$ )  $\delta$  = 9.50 (s, 1H, NH), 8.50 (s, 2H), 7.80 (d,  $J$  = 7.8 Hz, 2H), 7.67 (d,  $J$  = 7.6 Hz, 2H), 7.51 (t,  $J$  = 7.7 Hz, 2H), 7.29 (s, 2H), 7.18 (d,  $J$  = 4.7 Hz, 2H), 6.84 (d,  $J$  = 3.7 Hz, 2H), 6.78 (d,  $J$  = 4.5 Hz, 2H), 6.66 (s, 2H);  $^{13}\text{C}\{^1\text{H}\}$  NMR (126 MHz,  $\text{CDCl}_3$ )  $\delta$  = 173.9, 155.0, 148.3, 140.3, 135.7, 134.9, 134.8, 134.3, 134.0, 129.8, 129.7, 129.4, 128.0, 126.2, 124.7, 122.1, 110.2. UV/Vis/NIR ( $\text{CH}_2\text{Cl}_2$ ):  $\lambda_{\text{max}}/\text{nm}$  ( $\log \epsilon$  [ $\text{mol}^{-1} \text{dm}^3 \text{cm}^{-1}$ ]): 329 (4.88), 414 (4.69), 563 (4.40). MALDI-TOF:  $m/z$  calcd for  $\text{C}_{46}\text{H}_{20}\text{F}_{10}\text{N}_3\text{S}_2$ : 868.086  $[\text{M}+\text{H}]^+$ ; found: 868.108.

**Reduction of 3a:** A flame dried flask was charged with **3a** (20 mg, 0.026 mmol), degassed 6 ml THF and 3 ml methanol. Then,  $\text{NaBH}_4$  (9.90 mg, 0.260 mmol) was added, completion of the reaction was

monitored using TLC. The reaction was quenched with H<sub>2</sub>O (20 mL). The organic phase was extracted with CH<sub>2</sub>Cl<sub>2</sub> (2 x 20 ml) and the solvent was removed under reduced pressure to afford a dark blue semi-solid. The crude mixture was subjected to column chromatography, but it rapidly reverts back to its oxidized form. Hence, further characterization was hampered.

**Reduction of 3b** (20 mg, 0.023 mmol) was carried out by following the above procedure using NaBH<sub>4</sub> (8.80 mg, 0.260 mmol), giving similar results as the reduced forms are not stable.

## ASSOCIATED CONTENT

### Supporting Information

CCDC 1979328 (**2**), 1979329 (**3a**) contain the supplementary crystallographic data for this paper. These data can be obtained free of charge via [www.ccdc.cam.ac.uk/data\\_request/cif](http://www.ccdc.cam.ac.uk/data_request/cif). Characterization data (including HRMS, <sup>1</sup>H, and <sup>13</sup>C NMR spectra, further cyclic voltammograms and further computational results) absorption and single-crystal X-ray analyses of **2** and **3a**. The Supporting Information is available free of charge on the ACS Publications website.

## AUTHOR INFORMATION

### Corresponding Author

\*E-mail: gokul@iisertvm.ac.in

### ORCID

S. Gokulnath: 0000-0001-9299-5217

### Notes

The authors declare no competing financial interest.

## ACKNOWLEDGMENTS

S.G. thanks IISER Thiruvananthapuram for the facilities and SERB (Startup Grant No. SB/FT/CS-094/2014) and DST (Inspire Faculty Support IFA-CH-74) for funding. S.T. thanks CSIR and A.J. thanks DST-INSPIRE for their research fellowships. We thank Alex Andrews for solving the X-ray structures of **2** and **3a**.

## REFERENCES

- Stepień, M.; Latos-Grażyński, L. Benziporphyrins: Exploring Arene Chemistry in a Macrocyclic Environment. *Acc. Chem. Res.* **2005**, *38*, 88–98.
- (a) Lash, T. D. Carbaporphyrinoid Systems. *Chem. Rev.* **2017**, *117*, 2313–2446. (b) Szyszko, B.; Latos-Grażyński, L. Expanded Carbaporphyrinoids. *Angew. Chem. Int. Ed.* **2019**, *58*, 10.1002/anie.201914840. (c) Lash, T. D. Metal Complexes of Carbaporphyrinoid Systems. *Chem. - An Asian J.* **2014**, *9*, 682–705.
- (a) Sengupta, R.; Thorat, K. G.; Ravikanth, M. Synthesis of Nonaromatic and Aromatic Dithia Benzisapphyrins. *J. Org. Chem.* **2018**, *83*, 11794–11803. (b) Lash, T. D.; Yant, V. R. Improved Syntheses of *Meso*-Tetraarylbenzporphyrins and Observations of Substituent Effects on the Diatropic Characteristics of These Formally Nonaromatic Carbaporphyrinoids. *Tetrahedron* **2009**, *65*, 9527–9535. (c) Stepień, M.; Szyszko, B.; Latos-Grażyński, L. Steric Control in the Synthesis of *p*-Benziporphyrins. Formation of a Doubly N-Confused Benzihexaphyrin Macrocyclic. *Org. Lett.* **2009**, *11*, 3930–3933.
- (a) Chen, F.; Hong, Y. S.; Shimizu, S.; Kim, D.; Tanaka, T.; Osuka, A. Synthesis of a Tetrabenzotetraaza[8]circulene by a “Fold-In” Oxidative Fusion Reaction. *Angew. Chem. Int. Ed.* **2015**, *54*, 10639–10642. (b) Pawlicki, M.; Garbicz, M.; Szterenber, L.; Latos-Grażyński, L. Oxatriphyrins(2.1.1) Incorporating an ortho-Phenylene Motif. *Angew. Chem. Int. Ed.* **2015**, *54*, 1906–1909. (c) Adinarayana, B.; Thomas, A. P.; Yadav, P.; Mukundam, V.; Srinivasan, A. Carbatriphyrin(3.1.1)–A Distinct Coordination Approach of B<sup>III</sup> to Generate Organoborane and Weak C–H⋯B Interactions. *Chem. -Eur. J.* **2017**, *23*, 2993–2997. (d) Chen, F.; Kim, J.; Matsuo, Y.; Hong, Y.; Kim, D.; Tanaka, T.; Osuka, A. ortho-Phenylene-Bridged Hybrid Nanorings of 2,5-Pyrrolylenes and 2,5-Thienylenes. *Asian. J. Org. Chem.* **2019**, *8*, 994–1000. (e) Das, M.; Adinarayana, B.; Murugavel, M.; Nayak, S.; Srinivasan, A. Di-(*m-m*)terphenyl-Embedded Decaphyrin and Its Bis-Rh(I) Complex. *Org. Lett.* **2019**, *21*, 2867–2871.
- (a) Lash, T. D. Benziporphyrins, a Unique Platform for Exploring the Aromatic Characteristics of Porphyrinoid Systems. *Org. Biomol. Chem.* **2015**, *13*, 7846–7878. (b) Lash, T. D. Recent Advances on the Synthesis and Chemistry of Carbaporphyrins and Related Porphyrinoid Systems. *Eur. J. Org. Chem.* **2007**, *33*, 5461–5481. (c) Stepień, M.; Latos-Grażyński, L. Tetraphenyl-*p*-Benziporphyrin: A Carbaporphyrinoid with Two Linked Carbon Atoms in the Coordination Core. *J. Am. Chem. Soc.* **2002**, *124*, 3838–3839.
- Lash, T. D.; Chaney, S. T.; Richter, D. T. Conjugated Macrocycles Related to the Porphyrins. 12.1 Oxybenzi- and Oxyppyriporphyrins: Aromaticity and Conjugation in Highly Modified Porphyrinoid Structures. *J. Org. Chem.* **1998**, *63*, 9076–9088.
- (a) Berlin, K.; Breitmaier, E. Benziporphyrin, A Benzene Containing, Nonaromatic Porphyrin Analogue. *Angew. Chem., Int. Ed. Engl.* **1994**, *33*, 1246–1247. (b) Stepień, M.; Latos-Grażyński, L. Tetraphenylbenzporphyrin - A Ligand for Organometallic Chemistry. *Chem. - A Eur. J.* **2001**, *7*, 5113–5117.
- Corriu, R. J. P.; Bolin, G.; Moreau, J. J. E.; Vernhet, C. A Facile Synthesis of New Tetrapyrrole Macrocyclic Derivatives. Formation of Bimetallic Transition Metal Complexes. *J. Chem. Soc., Chem. Commun.* **1991**, 211–213.
- Ishida, M.; Kim, S. J.; Preihs, C.; Ohkubo, K.; Lim, J. M.; Lee, B. S.; Park, J. S.; Lynch, V. M.; Roznyatovskiy, V. V.; Sarma, T.; Panda, P. K.; Lee, C. H.; S. Fukuzumi, Kim, D.; Sessler, J. L. Protonation-Coupled Redox Reactions in Planar Antiaromatic *meso*-Pentafluorophenyl-Substituted *o*-Phenylene-Bridged Annulated Rosarins. *Nat. Chem.* **2013**, *5*, 15–20.
- (a) Stepień, M.; Sprutta, N.; Latos-Grażyński, L. Figure Eights, Möbius Bands, and More: Conformation and Aromaticity of Porphyrinoids. *Angew. Chem., Int. Ed.* **2011**, *50*, 4288–4340. (b) Saito, S.; Osuka, A. Expanded Porphyrins: Intriguing Structures, Electronic Properties, and Reactivities. *Angew. Chem., Int. Ed.* **2011**, *50*, 4342–4373. (c) Sessler, J. L.; Seidel, D. Synthetic Expanded Porphyrin Chemistry. *Angew. Chem., Int. Ed.* **2003**, *42*, 5134–5175.
- (a) Carré, F. H.; Corriu, R. J. P.; Bolin, G.; Moreau, J. J. E.; Vernhet, C. Aminosilanes in Organic Synthesis. Preparation of New Expanded Porphyrin Ligands and Bimetallic Transition-Metal Complexes. Crystal Structure of a Tetrapyrrole Macrocyclic Dirhodium Complex. *Organometallics* **1993**, *12*, 2478–2486. (b) Kumar, S.; Rao, M. R.; Ravikanth, M. Stable Core-Modified Doubly N-Fused Expanded Dibenziporphyrinoids. *J. Org. Chem.* **2018**, *83*, 1584–1590.
- Jeong, S. D.; Sessler, J. L.; Lynch, V.; Lee, C. H. Dithiabisapphyrin: A Core-Modified Sapphyrin Bearing

- Exocyclic Double Bonds at the *Meso*-Positions. *J. Am. Chem. Soc.* **2008**, *130*, 390–391.
- (13) Ajay, J.; Shirisha, S.; Ishida, M.; Ito, K.; Mori, S.; Furuta, H.; Gokulnath, S. Planar Antiaromatic Core-Modified 24 $\pi$  Hexaphyrin(1.0.1.0.1.0) and 32 $\pi$  Octaphyrin(1.0.1.0.1.0.1.0) Bearing Alternate Hybrid Diheterole Units. *Chem. - Eur. J.* **2019**, *25*, 2859–2867.
- (14) (a) Robertson, N. Catching the Rainbow: Light Harvesting in Dye Sensitized Solar Cells. *Angew. Chem., Int. Ed.*, **2008**, *47*, 1012–1014. (b) Wang, Y.; Kai, H.; Ishida, M.; Gokulnath, S.; Mori, S.; Murayama, T.; Muranaka, A.; Uchiyama, M.; Yasutake, Y.; Fukatsu, S.; Notsuka, Y.; Yamaoka, Y.; Hanafusa, M.; Yoshizawa, M.; Gakhyun, G.; Kim, D.; Furuta, H. Synthesis of a Black Dye with Absorption Capabilities Across the Visible-to-Near-Infrared Region: A MO-Mixing Approach via Heterometal Coordination of Expanded Porphyrinoid. *J. Am. Chem. Soc.* **2020**, *142*, 6807–6813. (c) He, B.; Zhrebetskyy, D.; Wang, H.; Kolaczowski, M.; Klivansky, L.; Tan, T.; Wang, L.; Liu, Y. Rational tuning of high-energy visible light absorption for panchromatic small molecules by a two-dimensional conjugation approach. *Chem. Sci.*, **2016**, *7*, 3857–3861. (d) Erten-Ela, S.; Yilmaz, D.; Icli, B.; Dede, Y.; Icli, S.; Akkaya, E. U. A Panchromatic Boradiazaindacene (BODIPY) Sensitizer for Dye-Sensitized Solar Cells. *Org. Lett.*, **2008**, *10*, 3299–3302.
- (15) (a) Banala, S.; Rühl, T.; Sintic, P.; Wurst, K.; Kräutler, B. “Blackening” Porphyrins by Conjugation with Quinones. *Angew. Chem., Int. Ed.*, **2009**, *48*, 599–603. (b) Y. Kage, S. Mori, M. Ide, A. Saeki, H. Furuta and S. Shimizu, *Mater. Chem. Front.*, **2018**, *2*, 112–120.
- (16) Jiao, C.; Zhu, L.; Wu, J. BODIPY-Fused Porphyrins as Soluble and Stable Near-IR Dyes. *Chem. - A Eur. J.*, **2011**, *17*, 6610–6614.
- (17) Ishiyama, T.; Takagi, J.; Yonekawa, Y.; Hartwig, J. F.; Miyaura, N. Iridium-Catalyzed Direct Borylation of Five-Membered Heteroarenes by *Bis*(pinacolato)diboron: Regioselective, Stoichiometric, and Room Temperature Reactions. *Adv. Synth. Catal.* **2003**, *345*, 1103–1106.
- (18) (a) Rath, H.; Sankar, J.; Praburaja, V.; Chandrashekar, T. K.; Joshi, B. S. Aromatic Core-Modified Twisted Heptaphyrins[1.1.1.1.1.1.0]: Syntheses and Structural Characterization. *Org. Lett.*, **2005**, *7*, 5445–5448. (b) Srinivasan, A.; Reddy, V. R. M.; Narayanan, S. J.; Sridevi, B.; Pushpan, S. K.; Ravikumar, M.; Chandrashekar, T. K. Tetrathia- and Tetraoxarubyrins: Aromatic, Core-Modified, Expanded Porphyrins. *Angew. Chem., Int. Ed.* **1997**, *36*, 2598–2601.
- (19) Kumar, S.; Thorat, K. G.; Ravikanth, M. Dibenzidecaphyrins (1.0.0.1.1.1.0.0.1.1) and their *Bis*-BF<sub>2</sub> Complexes. *J. Org. Chem.* **2018**, *83*, 14277–14285.
- (20) Kumar, S.; Ravikanth, M. Synthesis of Stable [28 $\pi$ ] *m*-Benzihexaphyrins (1.0.0.1.1.1). *J. Org. Chem.* **2017**, *82*, 12359–12365.
- (21) (a) Becke, A. D. J. A new mixing of Hartree-Fock and local density-functional theories. *J. Chem. Phys.* **1993**, *98*, 1372–1377. (b) Lee, C.; Yang, W.; Parr, R. G. Development of the Colle-Salvetti correlation-energy formula into a functional of the electron density. *Phys. Rev. B: Condens. Matter Mater. Phys.* **1988**, *37*, 785–789.
- (22) Ishiyama, T.; Takagi, J.; Yonekawa, Y.; Hartwig, J. F.; Miyaura, N. Iridium-Catalyzed Direct Borylation of Five-Membered Heteroarenes by *Bis*(pinacolato)diboron: Regioselective, Stoichiometric, and Room Temperature Reactions. *Adv. Synth. Catal.* **2003**, *345*, 1103–1106.
- (23) (a) Martina, S.; Enkelmann, V.; Wegner, G.; Schlüter, A.-D. *N*-Protected Pyrrole Derivatives Substituted for Metal-Catalyzed Cross-Coupling Reactions. *Synthesis*, **1991**, 613–615. (b) Zhong, Z.; Lin, G.-Q.; Sun, Z.-H.; Wang, B. *tert*-Butyl 2-borono-1*H*-pyrrole-1- carboxylate. *Acta Cryst.* **2009**, *E65*, 687.